Enhanced Cortical Thickness Measurements for Rodent Brains via Lagrangian-based RK4 Streamline Computation

Joohwi Lee[a], **Sun Hyung Kim**[b], **Ipek Oguz**[c], and **Martin Styner**[a,b]

[a]University of North Carolina at Chapel Hill, Department of Computer Science, United States

[b]University of North Carolina at Chapel Hill, Department of Psychiatry, United States

[c]The University of Iowa, Department of Electrical and Computer Engineering, United States

Abstract

The cortical thickness of the mammalian brain is an important morphological characteristic that can be used to investigate and observe the brain's developmental changes that might be caused by biologically toxic substances such as ethanol or cocaine. Although various cortical thickness analysis methods have been proposed that are applicable for human brain and have developed into well-validated open-source software packages, cortical thickness analysis methods for rodent brains have not yet become as robust and accurate as those designed for human brains. Based on a previously proposed cortical thickness measurement pipeline for rodent brain analysis,[1] we present an enhanced cortical thickness pipeline in terms of accuracy and anatomical consistency. First, we propose a Lagrangian-based computational approach in the thickness measurement step in order to minimize local truncation error using the fourth-order Runge-Kutta method. Second, by constructing a line object for each streamline of the thickness measurement, we can visualize the way the thickness is measured and achieve sub-voxel accuracy by performing geometric post-processing. Last, with emphasis on the importance of an anatomically consistent partial differential equation (PDE) boundary map, we propose an automatic PDE boundary map generation algorithm that is specific to rodent brain anatomy, which does not require manual labeling. The results show that the proposed cortical thickness pipeline can produce statistically significant regions that are not observed in the the previous cortical thickness analysis pipeline.

Keywords

cortical thickness; Laplace partial differential equation; rodent brain analysis; runge-kutta integration

---

1. INTRODUCTION

The development of other mammalian brain such as rodents has significant relationship with the development of the human brain. Experimental studies on normal and genetically altered rodents have revealed information and insights about the structure and the development of the cerebral cortex. Many of detailed information about the neuronal development of the

---

Further author information: (Send correspondence to Joohwi Lee.), joohwi@cs.unc.edu, Telephone: 1 919 728 1024.

cortex have been found by observing rodent brains.[2] Rodent models have allowed various experiments designed for the identification of factors such as toxic material and genetic patterns that affects the shape change and the development of their brains. Thus, the analysis of rodent brains has gained increasing interests[3–5] including the cortical thickness analysis for the rodent brain as well.

When compared to MRI-based human brain analysis, the analysis of rodent brain can be less complicated in two ways. First, the rodent cortex does not show complex folding patterns observed in human and primate brains so that the geometric processing of the rodent brain surface model can be simplified, for example, no need to use a surface inflation technique. A simpler geometric algorithm tends to perform more robust and consistent than a complicated algorithm. Second, the controlled environment and the identical genetic copy implemented in the design of rodent model experiments also reduce the natural variation of rodent brain. Several image processing algorithms perform better when the natural variation is minimized, for example, atlas-based segmentation. The analysis of rodent brain, therefore, can be less challenging than the analysis of human brain. However, such minimal variation may come to challenges in statistical analyses. Because the variation is so small compared to that of human brain, each of image and shape processing algorithm employed in the cortical thickness analysis pipeline should perform more robust, consistent, and accurate than the tools developed for human brain.

Automatic cortical thickness measurement methods for rodent brains have been developed previously[1, 6] based on the solution of the Laplace PDE; however, both of the current cortical thickness analysis pipelines proposed by Lerch et al., and Lee et al., have limitations in performing accurate cortical thickness analysis. First, the Laplace PDE-based thickness computation method employed in both of these methods cannot guarantee sub-voxel accuracy due to their voxel-based implementation. Because the solutions are optimized within the voxel grid and then integrated using the Euler method, the precision of the thickness measurement cannot be smaller than the voxel size. In order to achieve sub-voxel accuracy while minimizing numerical errors, we propose to compute the cortical thickness using the fourth-order Runge-Kutta (RK4) integration method within the space of the spherical harmonic point distribution model (SPHARM-PDM), which was employed for statistical analyses in Lee et al. The RK4 integration method is an adaptive multi-step integration method that minimizes local truncation error up to the order of $O(n^4)$ and thus is more accurate than the first-order Euler method used in the previous pipeline. The streamlines integrated by the RK4 method are then examined to perform a geometric post-processing that verifies whether the streamlines fit exactly at the inner and outer surfaces of the rodent cortex.

Second, the PDE-based thickness solution is sensitive to the definition of a PDE boundary label map, because the analytic solution is determined completely and uniquely by the Neumann and Dirichlet boundary conditions defined in the PDE boundary label map. Because an anatomically accurate and consistent PDE boundary map is the pre-condition for the subsequent Laplace PDE-based thickness computation step, the way to generate an anatomically consistent PDE boundary label map is crucial for Laplace PDE-based thickness computation. Thus, the generation of an anatomically consistent PDE boundary map is

clearly an important influential factor that must be assured in order to produce anatomically meaningful statistical results. However, both of the previous analysis pipelines generate the PDE boundary map via atlas-based segmentation method that propagates the PDE boundary map using the deformation field that was estimated by its underlying image registration method. Consequently, the PDE boundary map used in the previous pipelines is anatomically consistent only when the deformation field reflects correctly the anatomical relationship between the atlas and the subject, which is not always true. In fact, the previous cortical thickness analysis pipeline proposed by Lee et al.,[1] sometimes produced erroneous PDE boundary maps, and thereby either post-processing steps or manual correction steps were required in order to correct such propagation errors. The proposed automatic PDE boundary map generation algorithm does not depend on manually created PDE boundary maps. Instead, the PDE boundary map is directly created from the neocortex segmentation and the other sub-cortical structure segmentations by using surface-based label processing algorithms.

This paper is organized as follows. First, we provide background to understand the previous cortical thickness analysis pipeline and to contrast the differences between the previous pipeline and the proposed method. Although the thickness computation is the core of the pipelines, we first introduce the automatic PDE boundary map generation algorithm (Section 3.1), because the boundary map is provided as an input to the thickness computation step. Then, a numerically accurate RK4-based thickness computation method is described in Section 3.2, which produces thickness streamlines. Those streamlines are then post-processed in order to verify whether those streamlines are completely fit within the interior and exterior surfaces of the neocortex in order to achieve sub-voxel accuracy. The results are presented in Section 4.

2. PREVIOUS WORK

Taking measurements of the cortical thickness of the human brain from MRIs is challenging due to the highly convoluted structure of the cortex. Hence, several computerized thickness measurement methods have been proposed. The methods used to estimate cortical thickness for the human brain from MRIs are categorized into two types: surface-based and voxel-based.

The surface-based methods require the construction of a surface model for each interface, and most of these methods define thickness as the distance between two surfaces. The construction of such a surface model can differ for the various methods. For example, Fischl etl al.,[7] deformed the white matter (WM) boundary to the pial boundary and vice versa.[8] Alternatively, in the case where each boundary can be constructed independently, both boundaries can be deformed simultaneously by either snake-like deformable models[9] or level sets.[10] While maintaining the correspondence between two surfaces, the thickness is measured as the distance between the correspondence trajectories. These explicit surface models enable sub-voxel accuracy,[11] high sensitivity, and robustness for different field strengths, scanner upgrades, and scanner manufacturers. However, surface-based cortical thickness methods should employ methods to preserve the correct topology between two

surfaces, such as smoothness and self-intersection constraints or Laplacian functions, which require substantial computational costs.

In contrast, voxel-based methods are, in general, computationally efficient because they do not involve complex geometry processing for surfaces such as surface folding. However, the accuracy and precision of the thickness measurements is usually limited by the resolution of the voxel grid, which is affected by partial volume effects at low contrast boundaries. Voxel-based methods can be classified into morphological,[12, 13] line integral,[14] Laplacian,[15] and registration-based[16] approaches with several variations for each. For instance, Laplacian approaches solve the Laplace equation in different ways, such as boundary value relaxation[?] or matrix methods. The calculation of thickness also has several variations, such as summing the Euclidean distance from neighboring voxels on the same streamline or using Lagrangian initialization.

Both of the previous methods by Lerch et al.,[17] and Lee et al.,[1] employed atlas-based segmentation for the neocortex segmentation, followed by the boundary-solution label map generation to solve Laplace PDE. The measured thickness was sampled on top of the triangulated surface model reconstructed from the neocortex segmentation label. The main difference of the methods was the use of an explicit surface correspondence algorithm. Lerch et al., used implicit correspondence obtained from Laplace PDE, while Lee et al., employed a particle-based surface correspondence algorithm to establish group-wise surface correspondence, which better captures the surface correspondence using the principle-based information-theoretic cost function[18, 19] and therefore produces reliable statistical analysis results.

Figure 1 illustrates the steps for rodent brain cortical thickness analysis used in Lee et al.,.[1] The pipeline mainly consists of Laplace-PDE based thickness computation,[1, 6, 15] the SPHARM-PDM construction,[20] and the particle-based correspondence algorithm.[1, 18] The definition of thickness follows that of Jones et al.,,[15] which can be obtained from the solution of Laplace's equation. Laplace's equation is a second-order partial differential equation solved for a scalar field $u(\mathbf{x})$ that can be written as the form of $u = \nabla^2 u(\mathbf{x}) = 0$, where $u(\mathbf{x}) = u_L$ for $\mathbf{x} \in \Omega_{WM}$ and $u(\mathbf{x}) = u_H$ for $\mathbf{x} \in \Omega_{CSF}$. Ω_{WM} and Ω_{CSF} denote the WM-GM interface and the GM-CSF interface respectively. In order to reconstruct a surface model from the neo-cortex segmentation of each subject, the SPHARM description is used and, that is, a hierarchical, global, multi-scale boundary description that can only represent objects of spherical topology. Kelemen et al. demonstrated that SPHARM can be used to express shape deformations.[21] Truncating the spherical harmonic series at different degrees results in object representations at different levels of detail. SPHARM is a smooth, accurate fine-scale shape representation, given a sufficiently high representation level.

3. METHOD

3.1 Automatic PDE Boundary Map Generation

In order to correctly measure cortical thickness, a boundary condition map that defines the Laplace PDE boundary condition must be defined in an anatomically consistent manner. In the solution of Laplace PDE in my method, the solution domain is bounded by the Dirichlet

condition or the Neumann condition. While the Dirichlet condition defines values of the solution boundary as a constant, the Neumann boundary defines the values with the first order derivative of the solution. Hence, the interface with the Dirichlet condition defines the inner and the outer surface where streamlines start and arrive, and yet the Neumann condition defines an open boundary that is parallel to streamlines. Figure 2 shows the resulting Laplace PDE solution with the setting of different boundary conditions.

The PDE boundary definition map for a subject is defined within a label map. The creation of an accurate boundary map typically requires expert's assessment and quality control. In order to reduce time and labor cost, an atlas-based propagation is typically employed in that a single PDE boundary map is created for an atlas and then propagated towards each subject via the deformation field. Ideally, the propagation should produce a correct boundary map that is anatomically consistent with the subject, but in practice, the resulting boundary map is not accurate to reflect correct anatomical characteristics of the subject (See figure 7 on page 8).

When using the previous voxel-based approach,[1] a consistent boundary map generation only using voxel-based operations can be difficult because the PDE boundary map should be defined for surfaces. Thus, I propose surface-based pre-processing steps that can guarantee anatomically consistent PDE boundary map over subjects' surfaces. The preprocessing steps are illustrated in figure 3. First, the initial PDE boundary definition is converted from a voxel label into a point attribute of a SPHARM surface model. Each point attribute is copied from the closest voxel for the point. Second, a surface-based definition map is corrected via majority voting scheme. Assuming that each surface point is in correspondence, the majority voting based correction empirically has produced more consistent surface maps. Third, in order to compute the Laplace PDE solution in the voxel grid, a new boundary label map is created by computing a Voronoi map. Last, the solution domain is overlaid on top of the Voronoi map-based boundary map.

3.2 RK4-based Streamline Computation

After obtaining the Laplace PDE solution, the next step is the computation of the thickness between the interior (WM-GM) surface and the exterior (GM-CSF) surface. Following the definition of the Laplace PDE-based thickness, the thickness is measured by the length of a line between the two surfaces that satisfies the perpendicular condition: the line should be orthogonal to the isolines of the PDE solution at every point. The streamline is such a line that has the property of being tangent to the velocity field, the normalized gradient field of the PDE solution, at every point of the PDE solution. Thus, the streamline can be used as a mathematical analogy of the cortical column anatomy of the neocortex. The streamline also has a nice property of one-to-one correspondence between the WM-GM surface that is natural with respect to the neocortex anatomy.

The streamlines are calculated as follows. Let $d\mathbf{l}$ be a differential of length along a streamline as shown in Figure 5 on page 7. By definition of streamline, the infinitesimally small piece of curve $d\mathbf{l}$ should be parallel to the gradient vector $\nabla u = \left(\frac{\partial u}{\partial x}, \frac{\partial u}{\partial y}, \frac{\partial u}{\partial z} \right)$, that is,

$$
\mathrm{dl} \times \nabla \mathbf{u} \quad = \quad \left\{ \begin{array}{c} \mathrm{d}x \\ \mathrm{d}y \\ \mathrm{d}z \end{array} \right\} \times \left\{ \begin{array}{c} \frac{\partial u}{\partial x} \\ \frac{\partial u}{\partial y} \\ \frac{\partial u}{\partial z} \end{array} \right\} \quad = \quad \det \begin{vmatrix} \mathbf{i} & \mathbf{j} & \mathbf{k} \\ \mathrm{d}x & \mathrm{d}y & \mathrm{d}z \\ \frac{\partial u}{\partial x} & \frac{\partial u}{\partial y} & \frac{\partial u}{\partial z} \end{vmatrix} \quad = \quad 0. \quad (1)
$$

Expanding the determinant, the equation becomes

$$
\frac{\mathrm{d}}{\mathrm{d}x}\frac{\partial u}{\partial x} \quad = \quad \frac{\mathrm{d}}{\mathrm{d}y}\frac{\partial u}{\partial y} \quad = \quad \frac{\mathrm{d}}{\mathrm{d}z}\frac{\partial u}{\partial z}. \quad (2)
$$

In contrast to Euler's method used in the transport equation, The streamline is constructed explicitly by the integration of the vector field in a Lagrangian fashion. In order to minimize local truncation error and faster convergence, I solve the PDE using Runge-Kutta (RK) integration method. The fourth order RK method is the most popular numerical method and is highly accurate and explicit where cumulative error over a bounded interval is proportional to h^4. The Runge-Kutta update formula is given as

$$
X_{n+1} \quad = \quad X_n + \frac{h}{6}\left(k_1 + 2k_2 + 2k_3 + k_4\right), \quad (3)
$$

where

$$
k_1 \quad = \quad f\left(t_n, X_n\right), \quad (4)
$$

$$
k_2 \quad = \quad f\left(t_n, X_n + \frac{h}{2}k_1\right), \quad (5)
$$

$$
k_3 \quad = \quad f\left(t_n + \frac{h}{2}, X_n + \frac{h}{2}k_2\right), \quad (6)
$$

$$
k_4 \quad = \quad f\left(t_n + h, X_n + hk_3\right). \quad (7)
$$

3.3 Geometry Processing for Sub-voxel Accuracy

The explicit streamline geometry has several advantages. For example, the bundle of thickness streamlines provides intuitive visualization that allows biologists or pharmaceutical scientists to better understand the way the cortical thickness is measured. However, its most important feature is its ability to estimate thickness with sub-voxel accuracy. In analysis of the cortical thickness of the human brain, surface-based cortical thickness computation methods are shown to be more robust and consistent than voxel-based thickness computation methods,[22] because the thickness can be estimated directly using the surface-streamline relationship; that is, the streamline must start and finish at the inner and outer surfaces as defined. Figure 6 shows streamlines constructed via the voxel-based thickness computation using Euler method. In order to achieve sub-voxel accuracy, we process the starting and ending segments of the streamlines in order to fit them perfectly

within the boundary of the rodent neo-cortex. The enhancement via streamline geometry indeed shows much smoother thickness measurements than the voxel-based computation methods.

4. RESULTS

The proposed cortical thickness analysis pipeline demonstrates the use of the proposed registration and segmentation methods in the context of biomedical image analysis. This section addresses non-theoretical issues that may occur in the construction of an image and shape analysis pipeline, which may confound the results of analysis in significant ways.

4.1 The Effects of Registration Error

The proposed pipeline consists of several steps in which the processing results of one method are fed into the next method. During this streamlined processing, the pre-condition of each method must be met. For example, the boundary label map must be prepared for each subject in order to compute cortical thickness. The output of the thickness computation is sensitive to the input PDE-boundary label map in terms of whether the boundary label map is anatomically consistent or not. The use of segmentation by registration may result in such a boundary map that is not consistent with regard to anatomical features. Figure 7 on the following page presents the surface color maps that represent the inside and the outside boundary of the boundary map. The label propagated by the ANTs tool in (a) shows the geometric inconsistency between the label map and the surface model, whereas the label produced by the proposed segmentation method shows no such boundary inconsistency.

4.2 The Effects of Surface Correspondence Error

The proposed pipeline employs the particle-based surface correspondence algorithm proposed by Cates et al.[18] and Oguz et al.[23] Because the surface correspondence among surface models significantly impacts the statistical analysis results, for example, hypothesis test results for local thickness differences, the quality of the surface correspondence must be ensured to validate the results. In order to qualify the surface correspondence across subjects, the surface thickness map of subject *A* was transferred to the other subject *B*. If the surfaces of *A* and *B* are in correspondence, then surface thickness map *A* must show a similar surface thickness with the surface thickness of map *B*. Figure 8 shows the results of the surface thickness map propagation. Before performing the correspondence algorithm, the thickness pattern shown in the yellow box of Figure 8 (a) indicates possible correspondence error. The thin thickness pattern must be shown along the ridge line if the surface correspondence between *A* and *B* is consistent. This inconsistency was corrected after performing the correspondence algorithm as shown in Figure 8 (b). This example suggests the importance of establishing correspondence, among the surface models for statistical analysis.

5. CONCLUSION

In this paper, we proposed an enhanced cortical thickness analysis pipeline for rodent brains that was based on the previous cortical thickness analysis pipeline. The proposed pipeline

consisted of improved thickness computation using the RK4 method and a geometric post-processing algorithm. The computation time of the proposed thickness computation algorithm was shown to be inexpensive in comparison to the computation of the previous Euler-based thickness computation approach. The automatic PDE boundary map generation algorithm improved the robustness of the analysis pipeline by minimizing manual correction tasks and yet helps to produce an anatomically consistent boundary map. Finally, we compared the proposed pipeline and the previous pipeline in terms of the probability of significance and visualizations of the effects of the proposed components in the pipeline.

REFERENCES

[1]. Lee J, Ehlers C, Crews F, Niethammer M, Budin F, Paniagua B, Sulik K, Johns J, Styner M, Oguz I. Automatic cortical thickness analysis on rodent brain. SPIE Medical Imaging. Mar.2011 7962 796248–796248–11.

[2]. Bystron I, Blakemore C, Rakic P. Development of the human cerebral cortex: Boulder Committee revisited. Nature Reviews Neuroscience. Feb.2008 9:110–122. [PubMed: 18209730]

[3]. Badea A, Nicholls PJ, Johnson GA, Wetsel WC. Neuroanatomical phenotypes in the Reeler mouse. NeuroImage. Feb.2007 34:1363–1374. [PubMed: 17185001]

[4]. Ma Y, Hof PR, Grant SC, Blackband SJ, Bennett R, Slatest L, McGuigan MD, Benveniste H. A three-dimensional digital atlas database of the adult C57BL/6J mouse brain by magnetic resonance microscopy. Neuroscience. 2005; 135(4):1203–1215. [PubMed: 16165303]

[5]. Pitiot A, Pausova Z, Prior M, Perrin J, Loyse N, Paus T. Magnetic resonance imaging as a tool for in vivo and ex vivo anatomical phenotyping in experimental genetic models. Human Brain Mapping. Jun.2007 28:555–566. [PubMed: 17437283]

[6]. Lerch JP, Pruessner J, Zijdenbos AP, Collins DL. Automated cortical thickness measurements from MRI can accurately separate Alzheimer's patients from normal elderly controls. Neurobiology of …. 2008

[7]. Fischl B, Dale AM. Measuring the thickness of the human cerebral cortex from magnetic resonance images. Proceedings of the National Academy of Sciences of the United States of America. Sept.2000 97:11050–11055. [PubMed: 10984517]

[8]. Davatzikos C, Bryan N. Using a deformable surface model to obtain a shape representation of the cortex. IEEE transactions on medical imaging. 1996; 15(6):785–795. [PubMed: 18215958]

[9]. Kim JS, Singh V, Lee JK, Lerch J, Ad-Dab'bagh Y, MacDonald D, Lee JM, Kim SI, Evans AC. Automated 3-D extraction and evaluation of the inner and outer cortical surfaces using a Laplacian map and partial volume effect classification. NeuroImage. Aug.2005 27:210–221. [PubMed: 15896981]

[10]. Zeng X, Staib LH, Schultz RT, Duncan JS. Segmentation and measurement of the cortex from 3D MR images. Medical Image Computing and …. 1998

[11]. Fischl B, Dale a. M. Measuring the thickness of the human cerebral cortex from magnetic resonance images. Proceedings of the National Academy of Sciences of the United States of America. Sept.2000 97:11050–5. [PubMed: 10984517]

[12]. Measuring thickness from 3D gray-scale image by fuzzy distance transform. IEEE; 2011.

[13]. Lohmann G, Preul C, Hund-Georgiadis M. Morphology-Based Cortical Thickness Estimation. IPMI. 2003; 18:89–100.

[14]. Aganj I, Sapiro G, Parikshak N, Madsen SK, Thompson PM. Measurement of cortical thickness from MRI by minimum line integrals on soft-classified tissue. Human brain mapping. Oct.2009 30:3188–3199. [PubMed: 19219850]

[15]. Jones SE, Buchbinder BR, Aharon I. Three-dimensional mapping of cortical thickness using Laplace's Equation. Human Brain Mapping. Sept.2000 11:12–32. [PubMed: 10997850]

[16]. Das SR, Avants BB, Grossman M, Gee JC. Registration based cortical thickness measurement. NeuroImage. Apr.2009 45:867–879. [PubMed: 19150502]

[17]. Lerch JP, Carroll JB, Dorr A, Spring S, Evans AC, Hayden MR, Sled JG, Henkelman RM. Cortical thickness measured from MRI in the YAC128 mouse model of Huntington's disease. NeuroImage. Jun.2008 41:243–51. [PubMed: 18387826]

[18]. Cates J, Fletcher P, Styner M, Shenton M. Shape modeling and analysis with entropy-based particle systems. Processing in Medical. 2007:1–12. R.

[19]. Oguz I, Niethammer M, Cates J, Whitaker R, Fletcher T, Vachet C, Styner M. Cortical correspondence with probabilistic fiber connectivity. Information processing in medical imaging : proceedings of the … conference. Jan.2009 21:651–63. [PubMed: 19694301]

[20]. Styner M, Oguz I, Xu S, Brechbühler C, Pantazis D, Levitt JJ, Shenton ME, Gerig G. Framework for the Statistical Shape Analysis of Brain Structures using SPHARM-PDM. The insight journal (1071). 2006:242–250.

[21]. Kelemen A, Székely G, Gerig G. Elastic model-based segmentation of 3-D neuroradiological data sets. Medical Imaging, IEEE Transactions on. Oct.1999 18:828–839.

[22]. Li Q, Pardoe H, Lichter R, Werden E, Raffelt A, Cumming T, Brodtmann A. Cortical thickness estimation in longitudinal stroke studies: A comparison of 3 measurement methods. NeuroImage. Clinical. 2015; 8:526–535. [PubMed: 26110108]

[23]. Oguz, I.; Cates, J.; Fletcher, T.; Whitaker, R.; Cool, D.; Aylward, S.; Styner, M. Cortical correspondence using entropy-based particle systems and local features. Biomedical Imaging: From Nano to Macro, 2008. ISBI 2008; 5th IEEE International Symposium on; IEEE; 2008. p. 1637-1640.
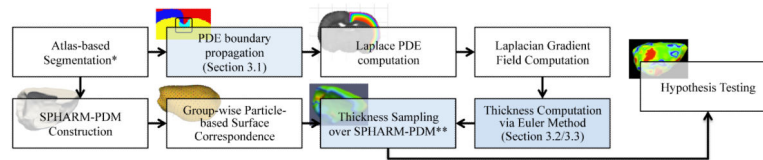
Figure 1.
The cortical thickness pipeline developed by Lee et al.,.[1] (1) First, the neo-cortex segmentation is created via atlas-based segmentation. (2) The PDE boundary map is provided with the atlas and propagated via the deformation field from the atlas-based segmentation. (3) The solution of Laplace PDE and (4) its gradient field is obtained within the voxel grid. (5) Thickness is computed by integrating the gradient field using Euler method and the measured thickness is sampled onto the SPHARM-PDM surface obtained from (6) and (7). The blue shaded steps are enhanced in the proposed method in order to improve accuracy and consistency. (* The atlas includes an intensity image, its structural segmentation label, and a manually created PDE boundary map. ** The sampling process is not necessary in the proposed method.
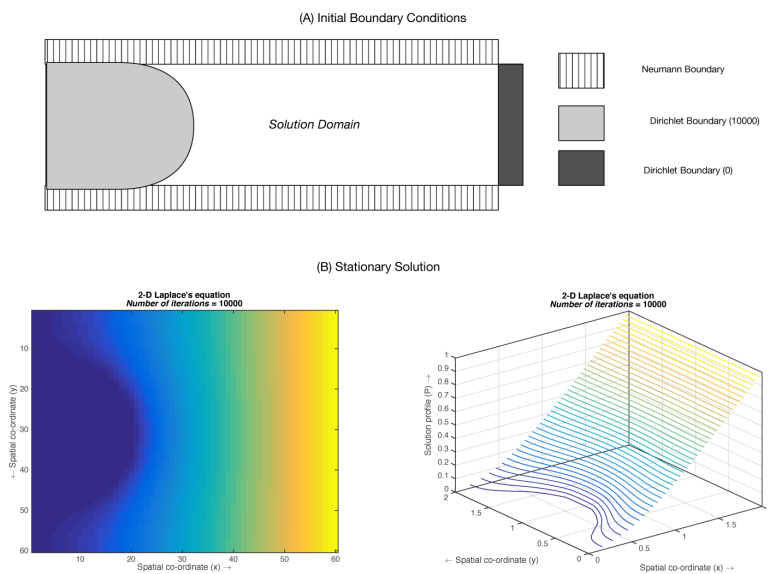
Figure 2.
A solution of Laplace equation is shown. A rectangular region is set up with two different boundary conditions (A). The Dirichlet boundary conditions are assigned at the curved left side and the flat right side of the rectangle. The curved Dirichlet boundary condition is assigned on the left side in order to show isolines parallel to the Dirichlet boundary (B). As seen in the color map and the contour images, the isolines are are parallel to the Dirichlet boundary and perpendicular to the Neumann boundary.
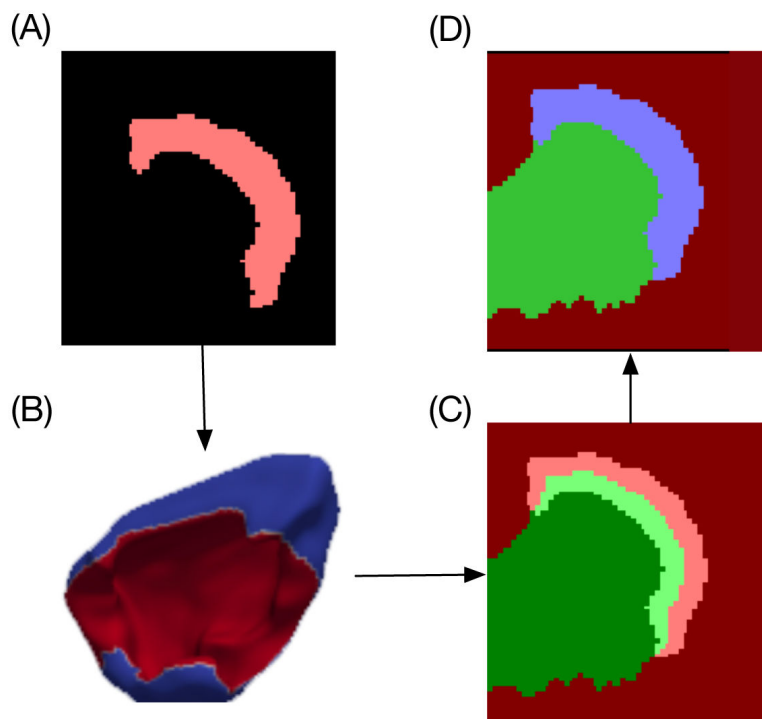
Figure 3.
Spatially consistent label map processing. (A) Initial segmentation label may contain minor segmentation errors during manual processing, which may cause erroneous thickness measurements. (B) I use a reconstructed surface model, where each point is associated with the inner or the outer surface labels, is constructed. An erroneous label surrounded by correct label values is removed by using such as a hole filling algorithm. (C) The correct surface model propagates a new boundary label map by computing a Voronoi map. (D) The final boundary map is generated by overlapping the original neocortex label on top of the Voronoi map.
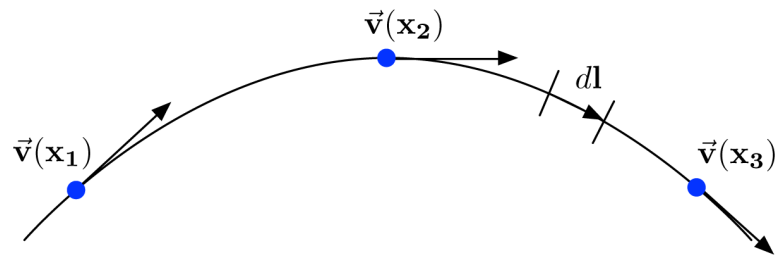
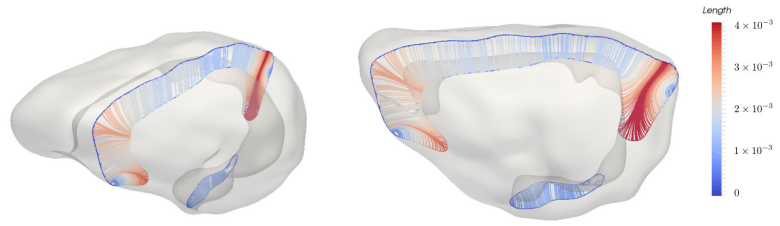**Figure 4.**
Streamline and differential of length.

Figure 5.
Streamline and differential of length.

(a) Voxel- vs. Surface-based   (b) Sub-voxel   (d) RK4-based Streamline
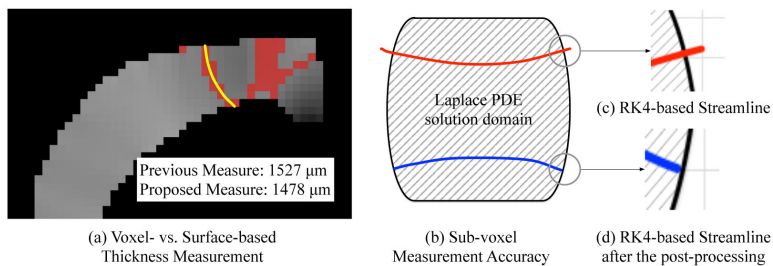Thickness Measurement   Measurement Accuracy   after the post-processing

Figure 6.
(a) The red voxels in the 2D gray axial slice image show streamlines measured by the voxel-based Euler method. The yellow line is the streamline constructed by the RK4 method. The voxel-based measurement is slightly greater than the RK4-based measurement. (b) Whereas the red streamline created by the RK4 method extends outside of the right surface due to the voxel size, the blue streamline is enhanced geometrically to fit exactly within the surface, which achieves sub-voxel accuracy.
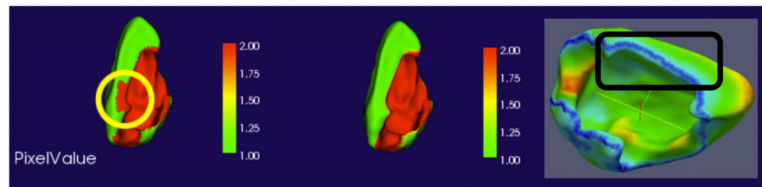
Figure 7.
Label propagation error possibly caused by registration error. (a) The label propagation errors are clearly shown around the ridges (yellow circles). (b) Segmentation by the proposed segmentation method. In (b), the label is consistent with the surface geometry features. The proposed segmentation method reduces the registration errors and therefore affects the computation of the cortical thickness. An example of boundary map difference between (a) and (b) is shown in (c). The surface color map (d) shows the incorrect computation of cortical thickness caused by the boundary map error.
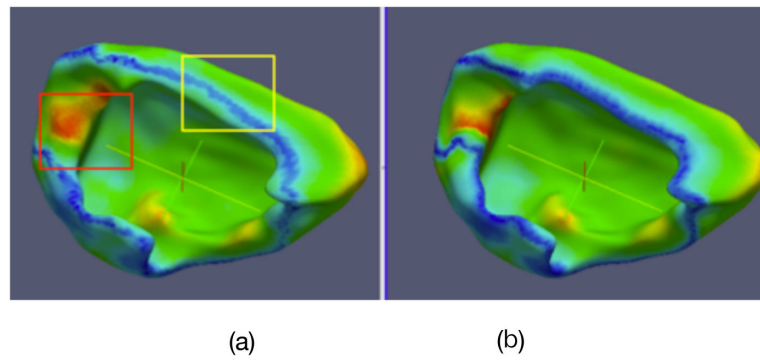
(a)   (b)

Figure 8.
The transferred surface thickness map of *A* is shown over the surface of subject *B* in (a). The thin blue band, which represents one of the thinnest cortex regions, is not shown on the ridge as it should be. The particle correspondence algorithm corrects such mis-correspondence so that the transferred surface map of *A* shows a similar thickness pattern over the surface of *B*, as seen in (b).